SIMULATION OF ECU FOR FLEXIBLE FUEL INJECTION SYSTEM IN SI ENGINE

Bui Van Ga[1], Nguyen Quang Trung[1], Le Minh Tien[1], Do Phu Nguu[2]*

[1]The University of Danang - University of Science and Technology, Vietnam
[2]The University of Danang - University of Technology Education, Vietnam

*Corresponding author: dpnguu@ute.udn.com

(Received: April 28, 2025; Revised: June 15, 2025; Accepted: June 20, 2025)

DOI: 10.31130/ud-jst.2025.23(9B).513E

Abstract - A hybrid renewable energy system utilizes an SI engine fueled by a syngas–biogas–hydrogen mixture with a wide range of compositional variations. Due to the significantly different stoichiometric air/fuel (A/F) ratios of these fuels, conventional fuel supply systems cannot meet the engine's operational requirements. Simulation results indicate that a 4 mm injector is suitable for biogas/hydrogen but not for syngas, whereas a 9 mm injector is appropriate for syngas but unsuitable for the other fuels. To handle the large variations in composition, a twinning injector system, consisting of two injectors, has been proposed. When the syngas content is low, only one injector operates; as the syngas proportion increases, the second injector is activated. This paper presents the simulation results of the ECU-controlled twinning injector system, along with experimental validation on a Honda GX390 engine.

Key words - HRES; Biogas; Syngas; Hydrogen; Flexible gaseous fuel engine

1. Introduction

Syngas and biogas are two types of biofuels derived from biomass through thermochemical and biochemical processes [1]. The typical volumetric composition of syngas includes 15–20% H_2, 15–20% CO, 1–5% CH_4, 10–15% CO_2, and the remainder is primarily N_2 [2]. When oxygen or steam is used as the oxidizing agent in the gasification furnace, the lower heating value (LHV) of syngas ranges from 10 to 28 MJ/Nm³. However, if air is used as the oxidizer, the LHV decreases to approximately 4–7 MJ/Nm³ [3]. Due to its low LHV, syngas-fueled engines generally exhibit lower power output compared to traditional fuels. Nevertheless, the air-to-fuel (A/F) ratio for stoichiometric combustion of syngas is approximately 1.2, significantly lower than that of gasoline (A/F = 14.9) or diesel (A/F = 14.5) [4-6], resulting in a power drop that is not directly proportional to the LHV. Typically, switching from diesel to syngas results in a power reduction of 15–20%, and 30–40% compared to gasoline-fueled engines [7, 8]. If the LHV of syngas is too low, unstable combustion may occur [9], which reduces engine efficiency. Thus, for effective operation in spark-ignition (SI) engines, the LHV of syngas must exceed 4.2 MJ/Nm³ [10].

Compared to syngas, biogas requires higher ignition energy, which can lead to misfiring and incomplete combustion in certain conditions, thereby reducing engine efficiency and increasing pollutant emissions [11]. The typical composition of biogas consists of 50–75% CH_4, 25–45% CO_2, 0–10% N_2, 1–2% H_2, and 0–2% O_2, with an LHV of around 25 MJ/Nm³ [12]. While CO_2 and N_2 reduce the calorific value, their presence enhances knock resistance and lowers combustion temperature, contributing to reduced NO_x formation [13].

Hydrogen is a carbon-free fuel characterized by a wide flammability range and high flame speed [14]. These properties enable hydrogen-fueled engines to achieve high in-cylinder pressures and temperatures while emitting no CO_2, CO, or hydrocarbons. Additionally, due to its wide flammability range, load control in hydrogen engines can be achieved by adjusting the equivalence ratio instead of the air–fuel flow rate [15]. This allows for simplification of throttle control mechanisms and eliminates the need for throttle position sensing. However, hydrogen also poses challenges such as low volumetric energy density, which reduces engine power output, and high combustion temperatures that increase NO_x emissions. Moreover, its low ignition energy and broad flammability range make it susceptible to abnormal combustion phenomena, including pre-ignition and backfire.

The significantly lower A/F ratio of syngas compared to conventional fuels presents a critical challenge for fuel delivery systems in engines. The low A/F results in extended injection durations, which may prevent complete induction of the fuel into the cylinder by the end of the intake stroke. Consequently, the engine may fail to achieve the theoretical stoichiometric equivalence ratio, particularly at high engine speeds. The accumulation of residual fuel in the intake tract from previous cycles further destabilizes equivalence ratio control in subsequent cycles. Therefore, for low A/F fuels like syngas, the mixing device must not only ensure a homogeneous fuel–air mixture but also guarantee complete induction of the entire fuel charge into the cylinder by the end of the intake process.

Until now, carburetion and port fuel injection (PFI) have been the most commonly employed methods for syngas fueling in spark-ignition (SI) engines [16]. Several studies on syngas carburetors have been conducted to achieve a homogeneous mixture suitable for various load conditions [17, 18]. Bui et al. designed a special mixing system to supply biogas-HHO to spark-ignition engines [19], and also for biogas fueling in SI engines retrofitted from diesel engines [20]. Currently, port fuel injection is widely applied for supplying gaseous fuels to SI engines, especially fuels containing hydrogen [21]. Since the mixture is formed in the intake manifold prior to induction

into the cylinder, the gaseous fuel occupies a significant portion of the mixture volume, leading to a reduced volumetric efficiency and, consequently, decreased engine power output [22], [23].

Direct injection of syngas into the combustion chamber is an effective solution to overcome the limitations of premixed systems [22]. The main technical challenge of direct-injection syngas engines is soot formation, which can clog the injector nozzle due to tar combustion. Furthermore, direct injection is more suitable for newly designed engines and is generally impractical for retrofitting conventional stationary SI engines originally designed for gasoline or CNG to operate on syngas-biogas-hydrogen mixtures.

To convert a conventional SI engine to operate on renewable gaseous fuels, several structural parameters must be adjusted to optimize working efficiency [13]. In intake systems for hydrogen-containing gaseous fuels, the injector should be positioned as close to the intake valve as possible [24]. For stationary engines, the injection timing and duration can be flexibly adjusted using potentiometers integrated with a specialized ECU [24]. When converting an electronically fuel-injected gasoline engine to gaseous fuel, the original ECU must be replaced with a programmable multifunction ECU [25]. Using this method, a single-cylinder Honda GX270 engine can be converted into a syngas-injected engine for power generation [26], or the Honda GX200 engine can be adapted for biogas-HHO fueling [27].

Injection pressure is a critical factor affecting mixture preparation. Commercially available gaseous fuel injectors can operate over a wide range of injection pressures. Typical LPG and CNG injectors for port-injection systems have a maximum injection pressure of 4 bar, with working pressures ranging from 1 to 3 bar [27]. Increasing fuel injection pressure tends to increase NO_x emissions [28]. For small two-stroke SI engines operating on CNG, the optimal injection pressure is less than 0.5 bar [29].

The above review indicates that syngas, biogas, and hydrogen each have unique advantages and limitations. Using them individually as engine fuels introduces several technical challenges. However, by appropriately blending these fuels, it is possible to harness the strengths of each, thereby improving engine performance. Although numerous studies have been published on syngas, biogas, hydrogen, or enriched syngas/biogas with CH_4 or H_2, very few have explored engines operating on combined syngas–biogas–hydrogen mixtures. Moreover, existing studies on fuel delivery systems primarily focus on supplying gaseous fuels with fixed compositions.

In this work, we present the design and experimental results of a port-injection fuel supply system for syngas–biogas–hydrogen mixtures, aimed at retrofitting conventional stationary SI engines to operate on flexible renewable gaseous fuels with significantly varying air–fuel (A/F) ratios.

2. Experimental Setup and Research Methodology

2.1. Engine and Fuels

The research was conducted on a Honda GX390 engine featuring a cylinder bore of 88 mm, piston stroke of 64 mm, and a compression ratio of 8.2. The original engine was gasoline-fueled, using a carburetor-based fuel supply system, and delivered a rated power output of 8.7 kW at 3600 rpm.

To investigate the impact of different fuel supply configurations on mixture formation, simulations were carried out using various injector nozzle diameters. Figure 1 illustrates the locations of the injectors installed on the intake manifold of the retrofitted engine.

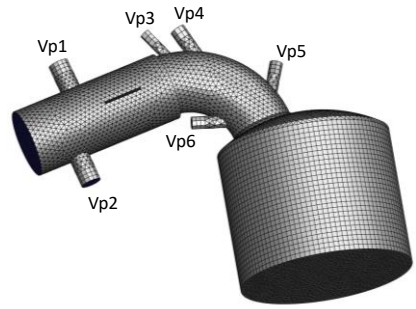

Vòi phun	dp(mm)
Vp1	9
Vp2	9
Vp3	4
Vp4	6
Vp5	5
Vp6	5

Figure 1. *Computational domain meshing and injector positions*

Due to a certain delay in injector opening, the injector control pulse must be triggered in advance to compensate for this lag. Moreover, sealing the injector for gaseous fuels is significantly more challenging than for liquid fuels. Therefore, if the injector orifice diameter is large, the injection pressure must be reduced to avoid gas leakage between the injector nozzle and its seat. The maximum injection duration per cycle depends on the engine speed and the ability of the intake process to draw the injected fuel completely into the cylinder. The key properties of biogas, syngas, and hydrogen are summarized in Table 1.

Table 1. *Fuel composition and properties*

Fuel	Composition (mol/mol)					V_{kk}/V_{nl} (l/l)
	CH_4	H_2	CO	CO_2	N_2	
Biogas	0.7	0	0	0.3	0	6.71
Syngas	0.05	0.18	0.20	0.12	0.45	1.39
Hydrogen	0	1	0	0	0	2.4
Blend 2 40B-40S-20H	0.3	0.272	0.08	0.168	0.18	3.72
Blend 9 50S-50H	0.025	0.59	0.1	0.06	0.225	1.9
Blend 14 50S-50B	0.375	0.09	0.1	0.21	0.225	4.05
LHV (MJ/Nm^3)	34	10	12	-	-	

2.2. Research Methodology

The study was conducted using simulations performed with the Ansys Fluent 2021R1 software. The computational domain includes the combustion chamber, cylinder, and intake manifold. The cylinder volume changes according to the crankshaft angle, so a dynamic mesh is applied to the cylinder space. The mesh division of the computational domain is shown in Figure 1. At the end of the intake process, the intake manifold is separated from the cylinder to reduce computational time.

The convection-diffusion governing equations are closed using the k-ε turbulence model. The thermodynamic

properties of the mixture are calculated using the Partially Premixed Combustion model. Each time the fuel is changed, the thermodynamic property table (PDF) is recalculated. This simplifies the boundary conditions for the calculation. At the intake inlet, only air is present, so the mixture fraction f is set to 0. At the nozzle inlet, only fuel is present, so f equals 1. The local equivalence ratio (ϕ) of the mixture is calculated through the fuel composition, oxygen content, or the mixture fraction f. The detailed process of model setup is presented in [9, 29].

The following section presents the simulation results for the formation of the mixture when injecting a syngas-biogas-hydrogen fuel blend and proposes a suitable fuel delivery method for engines using flexible gaseous fuels.

2.3. Experimental Investigation

The experiment was conducted on a GX 390 engine originally equipped with a carburetor, which was modified into a dual-injector fuel control system. The engine intake manifold was replaced with a steel pipe having a diameter equivalent to the original intake port. This modified intake system was equipped with two separate gaseous fuel injection lines, inclined at 60° relative to the intake direction, in order to form a homogeneous air-fuel mixture prior to entering the engine. Fuel injection was calculated and controlled along the intake path using two gas injectors, with interchangeable nozzle diameters of 4 mm, 6 mm, 8 mm, and 10 mm connected via corresponding fittings.

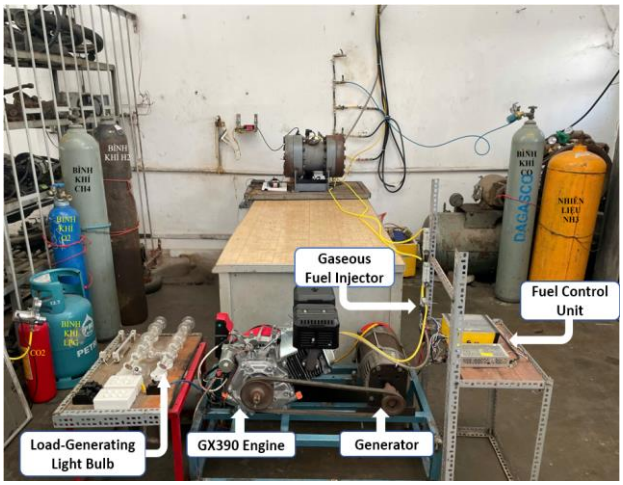

Figure 2. *Multi-fuel experimental setup on the GX390 engine*

The flow rate through the gaseous fuel injection valve was experimentally established by measuring the pressure differential before and after injection within the fuel chamber at a specified injection pressure over the actual control time. For nozzle diameters of 6 mm, 8 mm, and 10 mm, the experimental results indicated a linear relationship between fuel quantity and injection duration (Figure 3).

The flow rate through the gaseous fuel injector valve was experimentally determined by measuring the pressure differential across the injector before and after injection at a specified injection pressure over actual control time. For nozzle diameters of 6 mm, 8 mm, and 10 mm, the experiments confirmed a linear relationship between the injected fuel quantity and the injection duration, as illustrated in Figure 3.

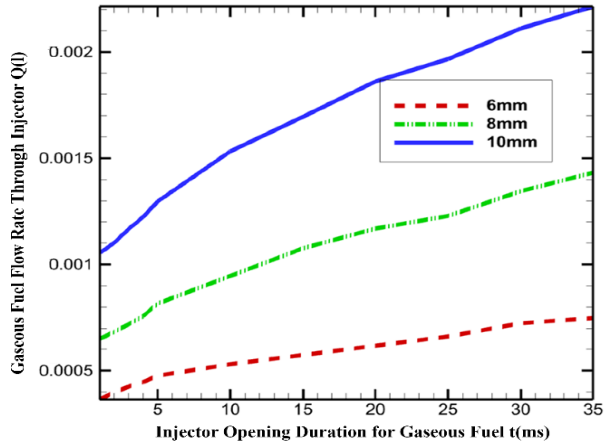

Figure 3. *Fuel Flow Characteristics of Injection Valves with 6 mm, 8 mm, and 10 mm Diameters*

3. Results and Discussion

3.1. Effect of Injector Diameter and Injection Pressure

Figure 4a presents the fuel concentration contours on the symmetric cross-section of the cylinder and intake manifold when the engine is fueled with syngas and running at 3000 rpm. The injection duration is set at 150°TK, with an injector hole diameter of 9mm and an injection pressure of 0.5 bar. When fuel injection begins at 10°TK, the pressure in the intake manifold increases locally, pushing a volume of air out of the intake pipe, causing negative airflow at the intake. However, immediately afterward, the airflow increases as the vacuum created in the cylinder during the piston downward stroke induces air intake. Under these conditions, the equivalence ratio in the compression stroke reaches 0.91, but a significant amount of fuel remains in the intake manifold at the end of the intake process. This fuel accumulation on the intake path can complicate the control of the equivalence ratio in subsequent cycles.

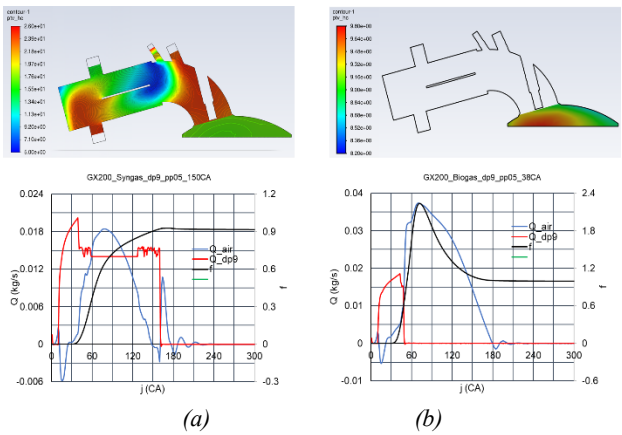

Figure 4. *Syngas and biogas injection were compared using a 9 mm diameter nozzle (n = 3000 RPM, pp = 0.5 bar) (a: Syngas, b: Biogas)*

In the same conditions of injection pressure and nozzle diameter, when biogas is injected, the injection duration only needs 38°TK to achieve an equivalence ratio of ϕ=1 (Figure 4b), and at the end of the intake stroke, all the injected fuel is drawn into the cylinder. The significant difference in the air/fuel ratio (Vair/Vfuel) between syngas

and biogas results in differences in injection duration and mixture formation conditions in the engine cylinder.

Figures 4a and 4b show that syngas and biogas enter the cylinder at nearly the same time (around 30°TK). However, the equivalence ratio curve for biogas increases sharply to a maximum value of ϕ=2 before gradually decreasing to a stable value. In contrast, the equivalence ratio curve for syngas increases slowly before stabilizing, due to the lower Vair/Vfuel ratio. The small Vair/Vfuel ratio is one of the major challenges for the fuel delivery system in engines using syngas.

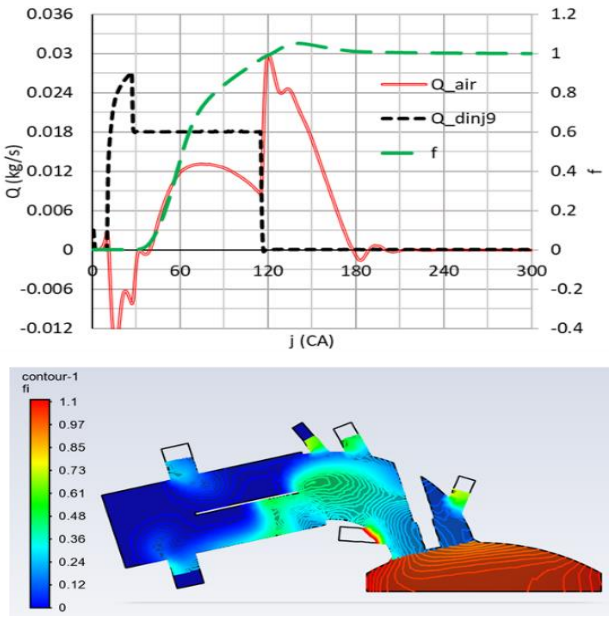

Figure 5. *Syngas injection through a 9 mm nozzle (pp = 1 bar, 105°CA spray duration) is characterized by fuel concentration contours, equivalence ratio and its variation, and flow rate as a function of crank angle*

To reduce the injection duration, the injection pressure can be increased. Figure 5 presents the simulation results of the mixture formation process for syngas when the injection pressure is increased to 1 bar, with a nozzle diameter of 9mm and an injection duration of 105°TK. The results show that the equivalence ratio of the mixture in the combustion chamber reaches ϕ=1; however, a significant amount of fuel remains in the intake pipe by the end of the intake stroke. Clearly, if this approach is applied for biogas injection, the injection duration would be very short, making it impossible to accurately control the injected fuel amount at low-load conditions. Furthermore, as discussed earlier, increasing the injection pressure with a large nozzle diameter presents significant challenges related to sealing the fuel nozzle for gaseous fuels. Therefore, using a large 9mm nozzle is not suitable for an engine utilizing the flexible syngas-biogas-hydrogen fuel mixture.

In cases where the fuel has a high Vair/Vfuel ratio, to extend the injection duration, a nozzle with a smaller hole diameter can be used. Figure 6a illustrates the injection process for hydrogen with a nozzle diameter of 4mm and an injection duration of 83°TK. With this injection duration, the fuel is completely drawn into the combustion chamber by the end of the intake stroke, and the equivalence ratio of the mixture reaches ϕ=1. However, under the same injection conditions, the equivalence ratio only reaches 0.12 for syngas (Figure 6b) and 0.6 for biogas (Figure 6c).

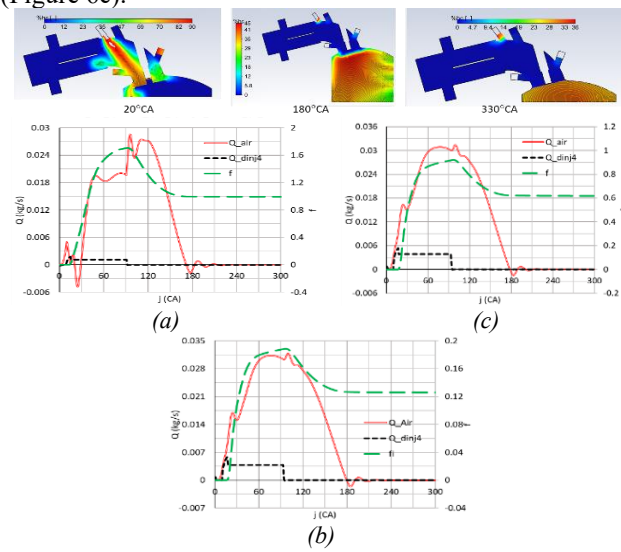

Figure 6. *Injection of hydrogen, syngas, and biogas was performed via a 4 mm diameter (dp) nozzle with an injection pressure (pp) of 1 bar and a spray duration (tp) of 83°CA*

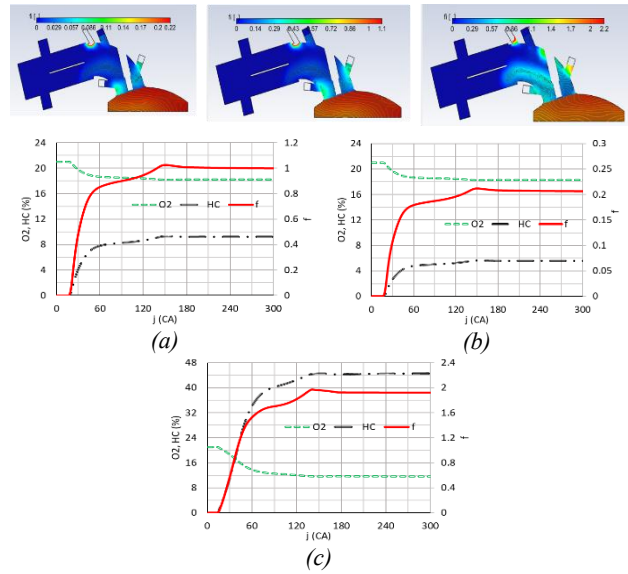

Figure 7. *Comparison of the mixing process of syngas, biogas, and hydrogen through the nozzle d_p=4mm, p_p=1bar, t_p=130 °TK*

At an injection duration of 130°CA, the equivalence ratio reaches f = 1 for biogas (Figure 7a), 0.2 for syngas (Figure 7b), and 1.7 for hydrogen (Figure 7c). However, incomplete fuel induction occurs at the end of the intake process for all fuels. Thus, with a nozzle diameter of d_p = 4 mm, the injection system is suitable for hydrogen but inadequate for biogas and syngas.

3.2. Effect of Injector Position

The injector position along the intake port influences the momentum of the fuel jet relative to the momentum of the intake air flow, thereby affecting the in-cylinder fuel concentration distribution. Figure 8 illustrates the fuel concentration contours and velocity fields in the intake port during Blend2 injection through injectors with diameters of

9 mm, 6 mm, and 5 mm, each placed at different positions.

The 9 mm injector is located at the entrance of the intake port. The 6 mm injector is positioned downstream of the throttle valve, directing the fuel jet toward the intake valve. The 5 mm injector directly sprays into the flow cross-section of the intake port during intake valve opening. The injection pressure is consistently maintained at 1 bar.

The 9 mm injector sprays perpendicularly to the port wall, causing the fuel jet to reflect and create a high-pressure region. This leads to a portion of the mixture escaping the intake port, which is subsequently drawn back in due to increased vacuum within the cylinder.

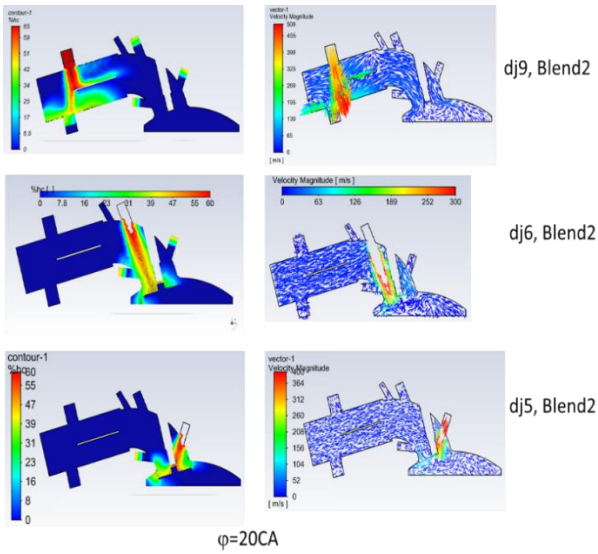

Figure 8. *Fuel concentration contours and velocity fields in the intake port were analyzed at 10°CA post-injection for Blend2 (n = 3000 RPM, pp = 1 bar)*

With the aforementioned injector positions and spray directions, it can be observed that by 10 °CA after the start of injection, the in-cylinder fuel concentration begins to increase in the cases of the 5 mm and 6 mm injectors, while in the case of the 9 mm injector, no fuel has entered the cylinder at that time. Figure 9 presents the evolution of equivalence ratio contours corresponding to the three injectors at crank angle positions of 90 °CA, 180 °CA, and 330 °CA.

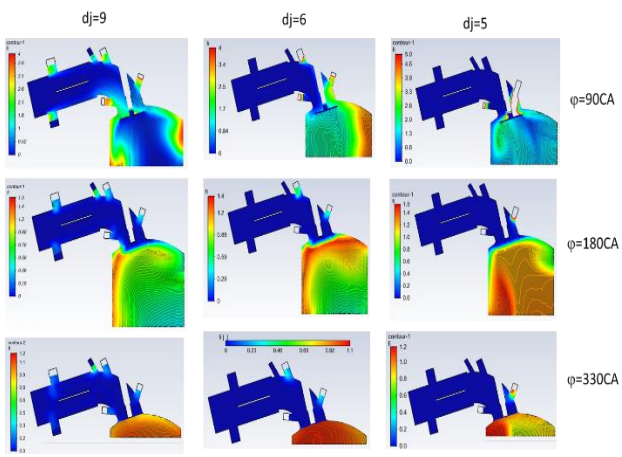

Figure 9. *Equivalence ratio contour evolution is shown for Blend2 injection via 9 mm (49°CA), 6 mm (72°CA), and 5 mm (110°CA) diameter nozzles and respective injection durations*

At 90 °CA, injection from the 9 mm and 6 mm nozzles has ended, whereas the 5 mm injector continues to inject. At this moment, for the 9 mm injector, regions of high equivalence ratio are located near the cylinder wall; for the 6 mm injector, high equivalence ratio regions are concentrated near the cylinder wall opposite the intake valve; and for the 5 mm injector, the equivalence ratio is relatively uniform throughout the cylinder.

At 180 °CA, the distribution of the equivalence ratio for the 9 mm case becomes more uniform compared to the others. However, the largest equivalence ratio gradient appears in the 5 mm injector case, where fuel tends to accumulate along the cylinder wall opposite the injector.

By 330 °CA, the mixture from the 6 mm injector is the most homogeneous; the 9 mm injector mixture becomes slightly leaner near the top of the combustion chamber, while the 5 mm injector results in a richer mixture concentrated along the chamber wall opposite the injector location.

The above results indicate that due to the significant differences in the air-to-fuel volume ratio V_{air}/V_{fuel} among syngas, biogas, and hydrogen, using a single injector with a fixed nozzle diameter is not suitable for all fuels. A large-diameter injector is appropriate for syngas but not for biogas and hydrogen. Conversely, a small-diameter injector works well with biogas and hydrogen but is unsuitable for syngas.

However, a single-injector system can be compatible with a syngas–biogas–hydrogen fuel blend when the syngas content is relatively low. When the injector is positioned close to the engine intake port, regions of high equivalence ratio tend to form along the combustion chamber wall opposite the injector. Although placing the injector at different locations along the intake port leads to variations in the fuel concentration distribution during the compression stroke, it does not significantly affect the overall mixture uniformity in the combustion chamber before ignition.

3.3. Effect of Injection Strategy

Syngas, biogas, and hydrogen can be injected separately through individual injectors (dual injection) or pre-mixed and delivered through a common injector (blend injection). Figure 10 presents the contour maps of CH_4, CO, HC, and equivalence ratio at crank angles of 20 °CA, 200 °CA, and 330 °CA for the case of separate injection of biogas and syngas. CH_4 is primarily present in biogas, while CO is predominantly found in syngas.

The results in Figure 10 show that during the compression stroke and prior to combustion, the in-cylinder distributions of CH_4, CO, and total hydrocarbons (HC) are similar. High-concentration fuel regions are located near the cylinder wall opposite the intake port. The local equivalence ratio within the combustion chamber varies from 0.9 to 1.12. Under these injection conditions, the overall equivalence ratio reaches ϕ=1, with a biogas/syngas ratio of 100%, equivalent to the Blend14 mixture (50% syngas and 50% biogas by volume).

It is observed that in dual injection, the biogas/syngas

ratio fluctuates significantly during the intake stroke. This is because biogas and syngas are injected separately through different injectors and thus enter the cylinder unevenly. When the syngas content is low, the biogas/syngas ratio increases sharply, leading to pronounced peaks in the ratio profile.

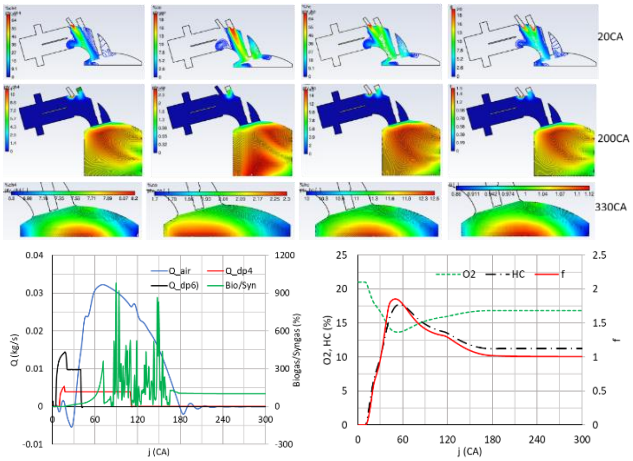

Figure 10. *Biogas injection via a 4 mm (100°TK) nozzle and syngas injection via a 6 mm (35°TK) nozzle were performed*

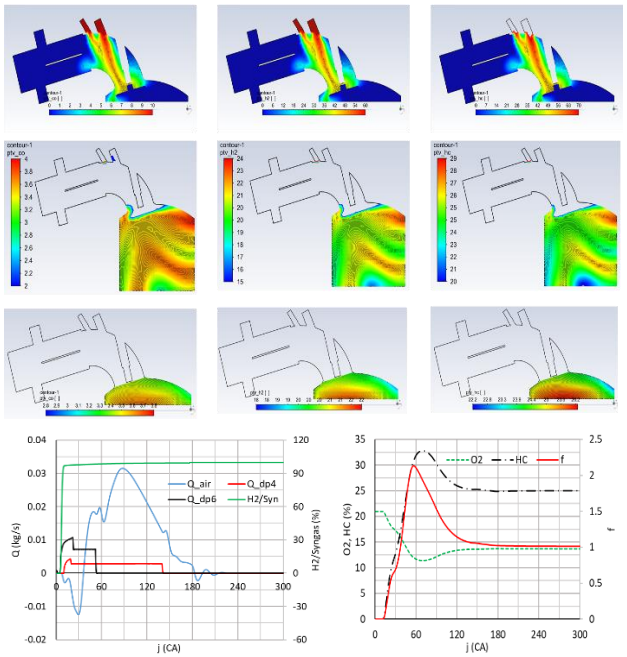

Figure 11. *Injection of a 50% syngas - 50% hydrogen blend via 4 mm (130°TK) and 6 mm*

In blend injection, the fuel mixture enters the cylinder as a homogeneous blend, so the proportion of each fuel component is fixed from the outset. Consequently, there is no notable difference in the spatial distribution of fuel components within the cylinder. Figure 11 illustrates the mixture formation process during the injection of a syngas–hydrogen blend. By the end of the compression stroke, the fuel-rich region is located near the piston crown, slightly shifted toward the intake side. The H_2/syngas ratio remains stable from the beginning as the blended fuel mixture enters the cylinder (Figure 11).

Figure 12 illustrates the mixture formation process when syngas and hydrogen are injected separately through 6 mm and 4 mm injectors, respectively. The hydrogen/syngas ratio fluctuates significantly during the intake stroke but becomes stable during the compression stroke. During compression, hydrogen tends to accumulate near the cylinder wall on the intake valve side. The variation in hydrogen concentration within the combustion chamber reaches 5%, ranging from a minimum of 19% to a maximum of 24%.

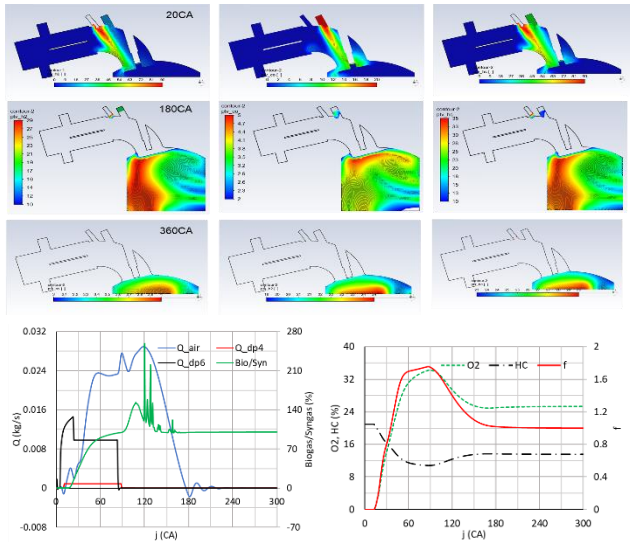

Figure 12. *Syngas was injected via a 6 mm (77°CA) nozzle concurrently with hydrogen injection via a 4 mm (77°CA) nozzle*

In contrast, for the blend injection case, the hydrogen concentration in the combustion chamber varies between 18% and 22%. Therefore, it can be concluded that for syngas–hydrogen fueling, the choice between blend and dual injection does not significantly affect the fuel concentration distribution within the combustion chamber.

3.4. Simulation of ECU for flexible fuel injection

The aforementioned research results enable the design of a specialized Electronic Control Unit (ECU) capable of delivering a flexible gaseous fuel mixture comprising syngas, biogas, and hydrogen to the engine. The fuel supply system consists of two injectors, whose injection durations are dynamically adjusted based on the composition of the fuel mixture. The longest injection duration corresponds to syngas. As the proportion of biogas or hydrogen in the mixture increases, the injection duration decreases accordingly. Figure 13 presents the ECU simulation schematic developed in Proteus. The ECU is implemented using an Arduino Mega microcontroller. Input signals include engine speed, load condition, and the composition ratios of syngas, biogas, and hydrogen. The embedded program within the microcontroller calculates the injection pulse width for each injector to ensure the correct quantity of fuel is delivered to the intake manifold.

In the simulation, the engine's operating conditions and fuel composition are represented by the positions of potentiometers. Relevant engine parameters, injection durations, and ignition timing are displayed on an LCD screen. The signals for Top Dead Center (TDC) position, ignition timing, and control pulses for both injectors are visualized using a virtual oscilloscope.

Figures 14a and 14b illustrate the results of the ECU

simulation program executed in Proteus. Each engine cycle contains two TDC (Top Dead Center) signals. The pulse interval between the intake and compression strokes is longer than that between the power and exhaust strokes. This distinction allows for programming the injection process to occur exclusively during the intake stroke, while ignition is triggered only at the end of the compression stroke, as shown in Figure 14b.

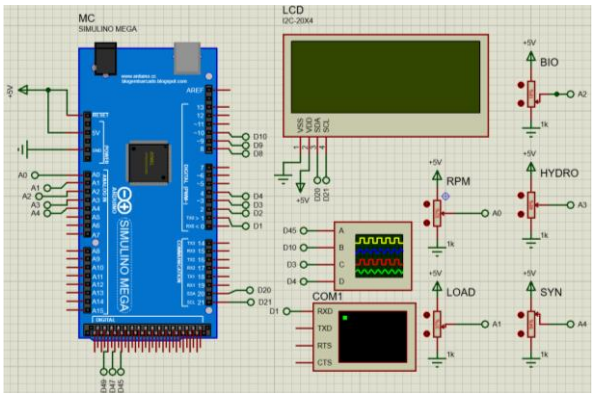

Figure 13. *Simulation of the ECU for controlling a flexible fuel injection system in an engine using Proteus*

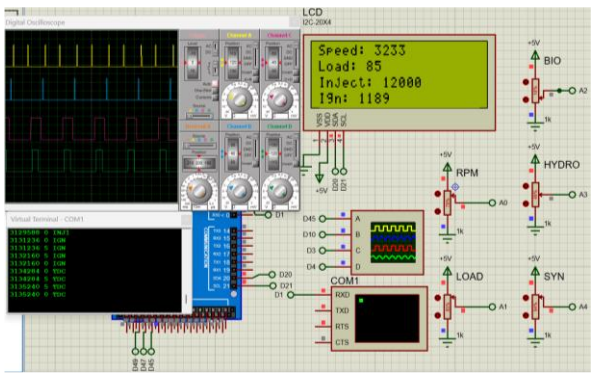

(a)

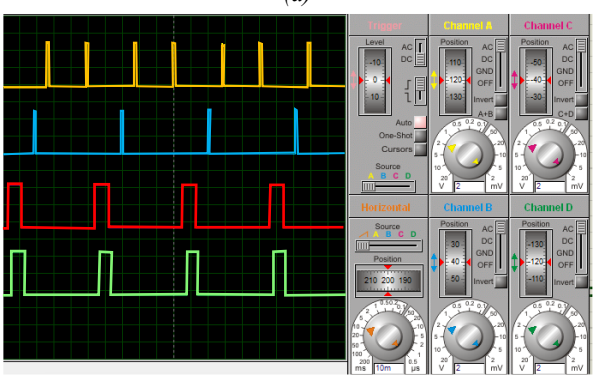

(b)

Figure 14. *Simulation results of the ECU program execution in Proteus*

3.5. Conversion of Honda GX390 engine to syngas-biogas-hydrogen flexible fuel engine

Based on the simulation results, a physical ECU was developed to control the flexible fuel supply system for a Honda GX390 engine. Figure 15a shows a photograph of the two injectors mounted on the intake manifold of the GX390 engine. These injectors are controlled by the ECU according to the program embedded in the microcontroller. Figure 15b presents an overview of the modified GX390 engine, which has been adapted to operate on a flexible fuel mixture of syngas, biogas, and hydrogen.

Figure 15. *Injector arrangement on the engine intake manifold (a) and overall view of the engine after modification for flexible fuel operation (b)*

Initial experimental results indicate that the ECU successfully controls the fuel supply process in accordance with the simulation outcomes. In future studies, we will conduct experimental measurements to evaluate the engine's performance characteristics and emission levels when operating on a syngas–biogas–hydrogen fuel mixture.

4. Conclusion

The findings of this study allow for the following conclusions:

- Using an injector with 4 mm nozzle diameter is suitable for biogas and hydrogen, but it is not appropriate for the syngas. Conversely, a 9 mm nozzle is well-suited for the syngas, but not for pure biogas or hydrogen.

- When injecting the syngas–biogas–hydrogen blend through injectors with diameters of 6 mm, the mixture distribution at 330 °CA is most homogeneous, but with 9 mm injector, the mixture is slightly lean near the top of the combustion chamber.

- When the injector is positioned near the intake valve, fuel-rich zones tend to form in the combustion chamber region opposite the spray direction.

- When injecting syngas and hydrogen separately through individual injectors, the hydrogen concentration in

the combustion chamber ranges from 19% to 24%, whereas in the blend injection case, it varies from 18% to 22%.

- A special ECU for supplying flexible syngas-biogas-hydrogen mixture can be simulated in Proteus and then manufactured to be used to convert a Honda GX390 engine into renewable fuel engine.

Acknowledgments: The authors wish to express their appreciation to the Ministry of Education and Training Vietnam for supporting this research under the project B2024.DNA.12, entitled "Smart controller for engine fueled with flexible gaseous fuels in hybrid renewable energy system".

REFERENCES

[1] R. Bates and K. Doelle, "Syngas Use in Internal Combustion Engines - A Review", *Advances in Research,* vol. 10, pp. 1-8, 01/10 2017.

[2] S. Gururaja Rao, S. H V, D. S, P. Paul, R. N K S, and H. Mukunda, "Development of producer gas engines", *Proceedings of The Institution of Mechanical Engineers Part D-journal of Automobile Engineering - PROC INST MECH ENG D-J AUTO,* vol. 219, pp. 423-438, 2005.

[3] H. FY, A. ARA, and S. SA, "Trends of syngas as a fuel in internal combustion engines", *Advances in Mechanical Engineering,* vol. 6, p. 401587, 2014.

[4] C. D. Rakopoulos and C. N. Michos, "Development and validation of a multi-zone combustion model for performance and nitric oxide formation in syngas fueled spark ignition engine", *Energy Conversion and Management,* vol. 49, no. 10, pp. 2924-2938, 2008.

[5] M. Christensen, A. Hultqvist, and B. Johansson, "Demonstrating the Multi Fuel Capability of a Homogeneous Charge Compression Ignition Engine with Variable Compression Ratio", *SAE Technical Papers,* vol. 108, 1999.

[6] B. D. Wood, *Applications of thermo-dynamics*, Addison-Wesley, 1982.

[7] Food and Agricultural Organization of the United Nation, *Wood gas as engine fuel*, FAO Forestry Department*,* 1986.

[8] U. Bossel, "Well-to-Wheel Studies, Heating Values, and the Energy Conservation Principle", *European Fuel Cell Forum,* 2003.

[9] S. Szwaja, V. B. Kovacs, A. Bereczky, and A. J. F. p. t. Penninger, "Sewage sludge producer gas enriched with methane as a fuel to a spark ignited engine", vol. 110, pp. 160-166, 2013.

[10] A. Shah, R. Srinivasan, S. D. F. To, and E. P. Columbus, "Performance and emissions of a spark-ignited engine driven generator on biomass based syngas", (in eng), *Bioresource technology,* vol. 101, no. 12, pp. 4656-4661, 2010.

[11] F. Y. Hagos, A. R. A. Aziz, and S. A. Sulaiman, "Methane enrichment of syngas (H2/CO) in a spark-ignition direct-injection engine: Combustion, performance and emissions comparison with syngas and Compressed Natural Gas", *Energy,* vol. 90, pp. 2006-2015, 2015.

[12] X. Kan, D. Zhou, W. Yang, X. Zhai, and C.-H. Wang, "An investigation on utilization of biogas and syngas produced from biomass waste in premixed spark ignition engine", *Applied Energy,* vol. 212, pp. 210-222, 2018.

[13] B. V. Ga, T. V. Nam, and T. T. Tung, "A Simulation of Effects of Compression Ratios on the Combustion in Engines Fueled With Biogas with Variable CO_2 Concentrations", *Journal of Engineering and Applications*, vol. 3, pp. 516-523, 2013.

[14] H. L. Yip *et al.*, "A Review of Hydrogen Direct Injection for Internal Combustion Engines: Towards Carbon-Free Combustion", *MDPI Journal,* vol. 9, no. 22, pp. 4842, 2019. https://doi.org/10.3390/app9224842

[15] R. Krishnaiah, S. Mathew, P. Bhasker, and E. Porpatham, "Gaseous alternative fuels for CI engines - a technical review", *International Journal of Pharmacy and Technology,* vol. 8, pp. 5257-5268, 2016.

[16] C. D. Rakopoulos, C. N. Michos, and E. G. Giakoumis, "Availability analysis of a syngas fueled spark ignition engine using a multi-zone combustion model", *Energy,* vol. 33, no. 9, pp. 1378-1398, 2008.

[17] S. Dasappa and H. V. Sridhar, "Performance of a diesel engine in a dual fuel mode using producer gas for electricity power generation", *International Journal of Sustainable Energy,* vol. 32, pp. 1-16, 2011.

[18] A. Kumar and A. Sharma, "Design and Development of Gas Carburettor for a Gasifier-Engine System", *Journal of The Institution of Engineers (India): Series C,* vol. 98, 2016.

[19] B. Van Ga, B. T. M. Tu, T. L. B. Tram, and B. Van Hung, "Technique of Biogas-HHO Gas Supply for SI Engine", *International Journal of Engineering Research and Technology,* vol. 8, no. 05, pp. 669-674, 2019.

[20] B. Van Ga, "Mixer Design for High Performance SI Engine Converted From A Diesel Engine", *International Journal of Engineering Research & Technology (IJERT, http://www.ijert.org),* vol. 3, pp. 2743-2760, 2014.

[21] S. J. Lee, H. S. Yi, and E. S. Kim, "Combustion characteristics of intake port injection type hydrogen fueled engine", *International Journal of Hydrogen Energy,* vol. 20, no. 4, pp. 317-322, 1995.

[22] F. Y. Hagos, A. R. A. Aziz, and S. A. Sulaiman, "Syngas (H2/CO) in a spark-ignition direct-injection engine. Part 1: Combustion, performance and emissions comparison with CNG", *International Journal of Hydrogen Energy,* vol. 39, no. 31, pp. 17884-17895, 2014.

[23] H. F. Yohaness, A.A.R. Aziz, S. A. Shaharin, and K. M. M. Bahaaddein, *Low and Medium Calorific Value Gasification Gas Combustion in IC Engines*, in Developments in Combustion Technology, 2016, Ch. 9.

[24] R. Hari Ganesh, V. Subramanian, V. Balasubramanian, J. M. Mallikarjuna, A. Ramesh, and R. P. Sharma, "Hydrogen fueled spark ignition engine with electronically controlled manifold injection: An experimental study", *Renewable Energy,* vol. 33, no. 6, pp. 1324-1333, 2008.

[25] F. Moreno, M. Muñoz, O. Magén, C. Monné, and J. Arroyo, "Modifications of a Spark ignition Engine to Operate with Hydrogen and Methane Blends", *Renewable Energy and Power Quality Journal,* vol. 1, pp. 421-426, 2010.

[26] G. Przybyla, A. Szlek, D. Haggith, and A. Sobiesiak, "Fuelling of spark ignition and homogenous charge compression ignition engines with low calorific value producer gas", *Energy,* vol. 116, pp. 1464-1478, 2016.

[27] V. G. Bui, V. N. Tran, A. T. Hoang, T. M. T. Bui, and A. V. Vo, "A simulation study on a port-injection SI engine fueled with hydroxy-enriched biogas", *Energy Sources, Part A: Recovery, Utilization, and Environmental Effects,* pp. 1-17, 2020.

[28] N. Bhange, P. Bansod, M. Hambarde, and S. Deodas, "Effects of CNG Injection Pressure on Performance, Emission and Combustion Characteristics of Multi-cylinder SI Engine", *International Journal of Recent Technology and Engineering (IJRTE),* vol. 8, pp. 2383-2387, 2019.

[29] M. Darzi, D. Johnson, C. Ulishney, and N. Clark, "Low pressure direct injection strategies effect on a small SI natural gas two-stroke engine's energy distribution and emissions", *Applied Energy,* vol. 230, pp. 1585-1602, 2018.